Title

Lupus Susceptibility Region Containing CDKN1B rs34330 Mechanistically Influences Expression and Function of Multiple Target Genes, Also Linked to Proliferation and Apoptosis

Journal

Arthritis & Rheumatology, 73(12)

ISSN

2326-5191

Authors

Singh, Bhupinder
Maiti, Guru P
Zhou, Xujie
et al.

Publication Date

2021-12-01

DOI

10.1002/art.41799

Peer reviewed

Arthritis & Rheumatology
Vol. 73, No. 12, December 2021, pp 2303–2313
DOI 10.1002/art.41799

American College of Rheumatology
Empowering Rheumatology Professionals

Lupus Susceptibility Region Containing *CDKN1B* rs34330 Mechanistically Influences Expression and Function of Multiple Target Genes, Also Linked to Proliferation and Apoptosis

Bhupinder Singh,[1] Guru P. Maiti,[1] Xujie Zhou,[2] Mehdi Fazel-Najafabadi,[1] Sang-Cheol Bae,[3] Celi Sun,[1] Chikashi Terao,[4] Yukinori Okada,[5] Kek Heng Chua,[6] Yuta Kochi,[7] Joel M. Guthridge,[1] Hong Zhang,[2] Matthew Weirauch,[8] Judith A. James,[1] John B. Harley,[8] Gaurav K. Varshney,[1] Loren L. Looger,[9] and Swapan K. Nath[1]

Objective. In a recent genome-wide association study, a significant genetic association between rs34330 of *CDKN1B* and risk of systemic lupus erythematosus (SLE) in Han Chinese was identified. This study was undertaken to validate the reported association and elucidate the biochemical mechanisms underlying the effect of the variant.

Methods. We performed an allelic association analysis in patients with SLE, followed by a meta-analysis assessing genome-wide association data across 11 independent cohorts (n = 28,872). In silico bioinformatics analysis and experimental validation in SLE-relevant cell lines were applied to determine the functional consequences of rs34330.

Results. We replicated a genetic association between SLE and rs34330 (meta-analysis $P = 5.29 \times 10^{-22}$, odds ratio 0.84 [95% confidence interval 0.81–0.87]). Follow-up bioinformatics and expression quantitative trait locus analysis suggested that rs34330 is located in active chromatin and potentially regulates several target genes. Using luciferase and chromatin immunoprecipitation–real-time quantitative polymerase chain reaction, we demonstrated substantial allele-specific promoter and enhancer activity, and allele-specific binding of 3 histone marks (H3K27ac, H3K4me3, and H3K4me1), RNA polymerase II (Pol II), CCCTC-binding factor, and a critical immune transcription factor (interferon regulatory factor 1 [IRF-1]). Chromosome conformation capture revealed long-range chromatin interactions between rs34330 and the promoters of neighboring genes *APOLD1* and *DDX47*, and effects on *CDKN1B* and the other target genes were directly validated by clustered regularly interspaced short palindromic repeat (CRISPR)–based genome editing. Finally, CRISPR/dead CRISPR-associated protein 9–based epigenetic activation/silencing confirmed these results. Gene-edited cell lines also showed higher levels of proliferation and apoptosis.

Conclusion. Collectively, these findings suggest a mechanism whereby the rs34330 risk allele (C) influences the presence of histone marks, RNA Pol II, and IRF-1 transcription factor to regulate expression of several target genes linked to proliferation and apoptosis. This process could potentially underlie the association of rs34330 with SLE.

INTRODUCTION

Systemic lupus erythematosus (SLE) is an inflammatory autoimmune disease characterized by autoantibody production, complement activation, and immune complex deposition, resulting in tissue and organ damage (e.g., in the kidney, skin, and lungs, among others). SLE incidence and prevalence has a strong sex bias (ratio of women to men 9:1) primarily affecting women of childbearing age, and a strong racial/ethnic bias, with a prevalence of SLE that is 3–5-fold higher in populations of Black, Hispanic, and Asian ancestries compared to those of White ancestry (1).

Genetic influence in SLE susceptibility is well established. Several genome-wide association studies (GWAS) have identified

Supported by the NIH (grants R01-AR-060366, R01-AI-132532, and R21-AI-144829 to Dr. Nath and grant P30-AR-073750 to Dr. James) and the National Research Foundation of the Republic of Korea (grant 2017M3A9B4050335 to Dr. Bae).

[1]Bhupinder Singh, PhD, Guru P. Maiti, PhD, Mehdi Fazel-Najafabadi, PhD, Celi Sun, MS, Joel M. Guthridge, PhD, Judith A. James, MD, PhD, Gaurav K. Varshney, PhD, Swapan K. Nath, PhD: Oklahoma Medical Research Foundation, Oklahoma City; [2]Xujie Zhou, MD, PhD, Hong Zhang, MD, PhD: Peking University First Hospital, Peking University, Ministry of Health of China, Beijing, China; [3]Sang-Cheol Bae, MD, PhD, MPH: Hanyang University Hospital for Rheumatic Diseases, Seoul, Republic of Korea; [4]Chikashi Terao, MD, PhD: RIKEN Center for Integrative Medical Sciences, RIKEN Yokohama Campus, Yokohama, Japan, and University of Shizuoka, Shizuoka, Japan; [5]Yukinori Okada, MD, PhD: Osaka University, Osaka, Japan; [6]Kek Heng Chua, PhD: University of Malaya, Kuala Lumpur, Malaysia; [7]Yuta Kochi, MD, PhD: Tokyo Medical and Dental University, RIKEN Center for Integrative Medical Sciences,

genetic associations between numerous single-nucleotide polymorphisms (SNPs) and SLE susceptibility (2). Among them, rs34330 was identified as a novel SLE susceptibility locus in East Asian populations (3). This SNP is located within the 5′-untranslated region (5′-UTR) (–79 C/T) of the cyclin-dependent kinase (CDK) inhibitor 1B gene (*CDKN1B*) at 12p13. *CDKN1B* encodes $p27^{Kip1}$, an inhibitor of cyclin/CDK complexes, which are crucial for cell cycle progression and development. *CDKN1B* plays a key role in many cellular events and can act as a tumor suppressor gene (4). The primary function of this multifunctional enzyme is to pause cell cycle progression during the G_1/S transition by inhibiting cyclin A/CDK2 activity until S phase onset (5), allowing cells to repair DNA damage and replication errors. Genetic lesions at *CDKN1B* could disrupt cell cycle control and contribute to cellular damage and SLE progression. Inhibitor $p27^{Kip1}$ localizes to multiple places in the cell. Its cell cycle functions are largely performed in the nucleus, whereas in the cytoplasm, it binds to the G protein RhoA, promoting apoptosis by inhibiting both p27 and RhoA (6). *CDKN1B* is also involved in autophagy modulation and autoimmunity development (7). The roles of $p27^{Kip1}$ in T cell function are complex. It opposes the development of CD4+ T cell effector function, inhibits proliferation of thymic and mature T cells, promotes T cell anergy and immune tolerance, and is critical for autophagy and apoptosis (7). In turn, autophagy promotes T cell proliferation through T cell receptor–driven degradation of $p27^{Kip1}$ (8).

The *CDKN1B* polymorphism at rs34330 has also been associated with susceptibility to multiple cancers including breast, lung, thyroid, endometrial, and hepatocellular cancer, where T is a risk allele (9). *CDKN1B* signaling promotes apoptosis in SLE patients undergoing bone marrow mesenchymal stem cell transplantation (10).

Since the first report, no study has been conducted to replicate rs34330 association with SLE, establish rs34330 target genes, or determine specific mechanisms and downstream genes by which rs34330 contributes to SLE susceptibility. In this study, using a combination of in vitro experimental assays in 3 SLE-relevant cell lines, we extensively characterized the impact of the rs34330 risk allele on *CDKN1B* and its neighboring genes. Our findings support the notion that the risk allele elevates cell type–specific promoter and enhancer activity, influencing the expression of multiple neighboring genes. Using clustered regularly interspaced short palindromic repeat (CRISPR)–based genetic and epigenetic editing, we validated and extended the predicted effects on target gene expression, proliferation, and apoptosis.

MATERIALS AND METHODS

Study design. The overall study design and experimental steps are outlined in Figure 1. First, to assess the consistency and veracity of the genetic effect, we performed an allelic association analysis with new cohorts followed by a meta-analysis of rs34330 (*CDKN1B*) across 11 independent cohorts of Asian and European ancestries (n = 28,872). Second, we used in silico bioinformatics analysis to identify potential regulatory effects on gene expression and annotated this region with epigenetic data on histone modifications and expression quantitative trait loci (eQTLs) across multiple tissues. Third, we performed luciferase reporter assays in the cell lines HEK 293 (kidney-derived neuronal), Jurkat (T lymphocyte), U937 (monocyte), and lymphoblastoid cell lines (LCLs) (lymphoblastoid B cells) to measure allele-specific regulatory effects. Fourth, a combination of DNA pull-down, electrophoretic mobility shift assay (EMSA), Western blotting, and mass spectrometry was used to identify DNA-bound proteins followed by chromatin immunoprecipitation (ChIP)–quantitative polymerase chain reaction (qPCR) to identify allele-specific binding of interacting proteins. Fifth, using chromosome conformation capture assays, we assessed chromatin interaction between rs34330 and neighboring genes in primary B cells, T cells, HEK 293 cells, and Jurkat cells. Sixth, CRISPR-based deletion and activation/inhibition were performed to assess SNP effects on target gene expression. Finally, we compared cell growth and viability between 35 nucleotide-edited knockout (KO) and wild-type (WT) cells using proliferation and apoptosis assays.

The methods discussed below are described in further detail in Supplementary Materials and Methods, available on the *Arthritis & Rheumatology* website at http://onlinelibrary.wiley.com/doi/10.1002/art.41799/abstract.

Assessment of rs34330 association with SLE. To assess the genetic association between rs34330 and SLE, we performed a meta-analysis using METAL (11) to assess GWAS data from 11 cohorts. We used summary statistics from the original 6 cohorts (12) (Supplementary Table 1, available on the *Arthritis & Rheumatology* website at http://onlinelibrary.wiley.com/doi/10.1002/art.41799/abstract) as the discovery cohort. To replicate the association with SLE, we genotyped rs34330 in 4 independent cohorts of Beijing Han Chinese (BHC), Korean, Malayan Chinese, and European-American ancestries (Supplementary Table 1) and added genetic data from a Japanese cohort (13). Association analysis and summary statistics for the genotyped SNPs were performed using Plink (14).

RIKEN Yokohama Campus, Yokohama, Japan; [8]Matthew Weirauch, PhD, John B. Harley, MD, PhD: Cincinnati Children's Hospital Medical Center, University of Cincinnati, and Cincinnati VA Medical Center, Cincinnati, Ohio; [9]Loren L. Looger, PhD: Howard Hughes Medical Institute, Janelia Research Campus, Ashburn, Virginia.

Drs. Singh and Maiti contributed equally to this work.

No potential conflicts of interest relevant to this article were reported.

Address correspondence to Swapan K. Nath, PhD, Oklahoma Medical Research Foundation, Arthritis and Clinical Immunology Program, 825 Northeast 13th Street, Oklahoma City, OK 73104. Email: swapan-nath@omrf.org.

Submitted for publication August 26, 2020; accepted in revised form May 4, 2021.

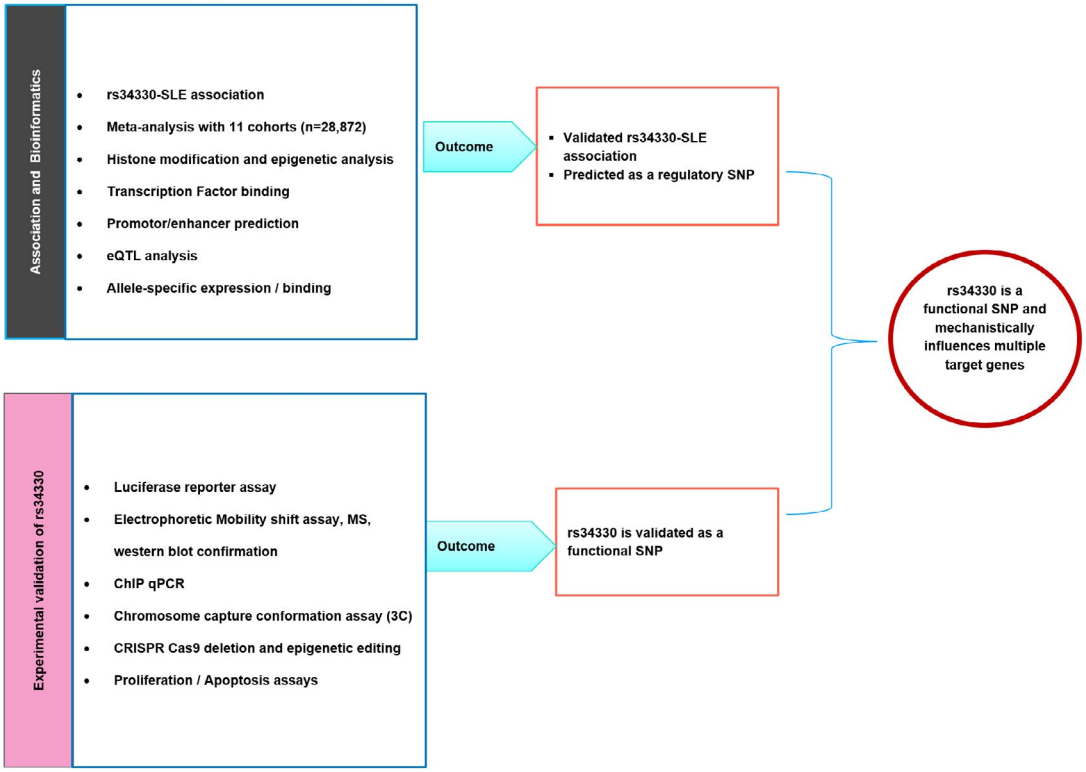

Figure 1. Overall study design and experimental steps to validate the association between rs34330 and systemic lupus erythematosus (SLE). eQTL = expression quantitative trait locus; SNP = single-nucleotide polymorphism; MS = mass spectrometry; ChIP = chromatin immunoprecipitation; qPCR = quantitative polymerase chain reaction; CRISPR = clustered regularly interspaced short palindromic repeat; Cas9 = CRISPR-associated protein 9.

Bioinformatics, transcription factor binding, and allelic imbalance analyses. To identify functional roles of the rs34330 region, we first used annotations from HaploReg-version 4.1 (15), and Bayesian functional scores from 3DSNP (16) and RegulomeDB (17). To assess chromatin context and epigenetic regulation at this locus, we identified several active histone marks (H3K27ac, H3K4me1, and H3K4me3), DNase I hypersensitivity, and RNA polymerase II (Pol II) binding for lymphoblastoid B cells (GM12878), using data from the ENCODE database (18) (Figure 2A).

Expression QTL analysis. To determine the effects of the rs34330 region on the expression of *CDKN1B* and neighboring genes, we assessed its effect in multiple tissue samples from the Genotype-Tissue Expression Project (19), LCLs from the Multiple Tissue Human Expression Resource project (18), and blood cell lines from Blood eQTL (20). We also queried whole blood–based eQTL data from the East Asian eQTL mapping project (21) and a Korean eQTL database for Crohn's disease (22). Additionally, we used a conditional eQTL database, which distinguishes between dependent and independent eQTL effects (23).

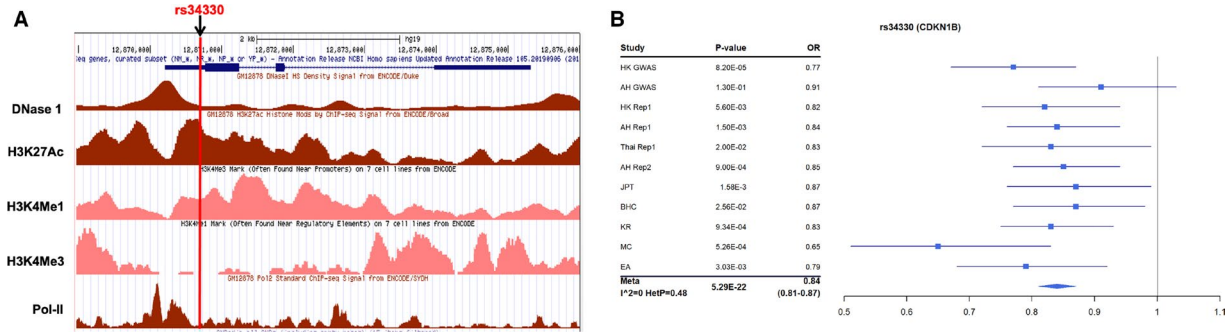

Figure 2. Genetic association between the single-nucleotide polymorphism rs34330 and systemic lupus erythematosus (SLE). **A**, ENCODE project data showing relevant histone marks, DNase I hypersensitivity, and RNA polymerase II (Pol II) binding in lymphoblastoid B cells (GM12878), with data obtained using the UCSC genome browser. **B**, Meta-analysis (Meta) and forest plots of association between rs34330 and SLE in the 11 cohorts of Asian and European ancestries. Squares represent the odds ratio (OR), and horizontal lines represent the 95% confidence interval. The elongated diamond represents the overall OR for the 11 cohorts. HK = Hong Kong; GWAS = genome-wide association study; AH = Anhui; Rep1 = replication 1; Thai = Thailand; JPT = Japanese in Tokyo; BHC = Beijing Han Chinese; KR = Korean; MC = Malayan Chinese; EA = European American.

Luciferase reporter assay. To assess the potential enhancer/promoter activity of this rs34330-containing region, we used the Dual-Luciferase Reporter Assay system (Promega). Briefly, the rs34330-containing region was cloned into the pGL4.26 vector for enhancer assay and the pGL4.14 vector for promoter assay (both from Promega). Each plasmid was transiently cotransfected with pGL4.74 (internal control) in HEK 293 cells, Jurkat cells, U937 cells, and LCLs. After 24 hours, enhancer/promoter activity was measured using a Dual-Luciferase Reporter Assay.

DNA pull-down assay. A DNA pull-down assay was performed as previously described (24). Briefly, nuclear extract from cultured Jurkat cell lines was incubated with biotin-labeled DNA (risk and non-risk alleles of rs34330) attached to Dynabeads M-280. Proteins bound to the beads were separated from unbound proteins by successive washes and later resolved with sodium dodecyl sulfate–polyacrylamide gel electrophoresis, followed by peptide mass fingerprint matrix-assisted laser desorption ionization mass spectrometry analysis of single bands.

ChIP assay. Two Coriell cell lines with the risk (CC) and non-risk (TT) genotypes for rs34330 were cultured in RPMI 1640 medium, and ChIP assays were performed using a Magnify ChIP kit (Invitrogen). Briefly, 1×10^7 cells were fixed, sonicated, and immunoprecipitated against targeted antibodies (poly[ADP-ribose] polymerase [PARP-1], interferon regulatory factor 1 [IRF-1], CCCTC-binding factor [CTCF], Pol II, H3K27ac, H3K4me3, and H3K4me1). DNA from the immunoprecipitated chromatin complexes was eluted, reverse crosslinked, purified, and later subjected to quantitative reverse transcriptase–PCR (qRT-PCR) analysis.

Chromosome conformation capture assay. Chromosome conformation capture is an important technique used to study chromatin structures that occur in living cells. Briefly, together with primary T cells and B cells, HEK 293 and Jurkat cells were fixed with formaldehyde, and crosslinked nuclei were isolated after cells were lysed. The nuclear content was digested with *Sac* I and T4 DNA ligase. The digested DNA was purified by proteinase K digestion, followed by phenol–chloroform treatment and alcohol precipitation. The purified DNA was diluted for chromosome conformation capture–PCR after quantitation.

CRISPR/CRISPR-associated protein 9 (Cas9)–based deletion of the rs34330 region. We used CRISPR/Cas9 to delete a small region (<40 bases) surrounding rs34330 in 2 different cell lines (HEK 293 and Jurkat). Briefly, to deliver the single-guide RNA (sgRNA)/Cas9 RNP complex into HEK cells, we used Lipofectamine 3000, and a Neon Electroporation system was used for Jurkat cells. After 4 days and 7 days, indel efficiency was measured using Sanger sequencing, and analyzed using TIDE and/or ICE. For downstream experiments, CRISPR-edited pooled cells were grown, harvested, and later subjected to messenger RNA isolation and quantitative PCR for *CDKN1B* and neighboring genes *DDX47*, *APOLD1*, *MANSC1*, and *GPR19*.

CRISPR-based activation and CRISPR inhibition. For CRISPR inhibition and CRISPR-based activation, plasmids SP-dCas9-VPR (no. 63798), pcDNA-dCas9-p300 (no. 61357), and dCas9-KRAB-MeCP2 (no. 110821) (all from Addgene; kind gifts from Dr. George Church, Harvard Medical School, Boston, MA) (25–27) were used. The pools of sgRNA were the same as those used for the Cas9 deletion experiment. Transfections in HEK 293 cells were performed in 24-well plates using 375 ng of respective dead Cas9 (dCas9) expression vector and 125 ng of equimolar-pooled or individual guide RNA expression vectors mixed with Lipofectamine 3000 (no. L300001; Life Technologies). Cells were harvested for RNA 72 hours post-transfection. RNA was extracted, and qPCR was performed as previously described (24).

Flow cytometric analysis of cell apoptosis. KO and WT Jurkat cells were stained with Ki-67 for proliferation assays. Apoptosis between 2 groups of cell lines (KO and WT) was also measured after cells were maintained under serum starvation conditions for 2 hours. The progression of the cell cycle was measured using propidium iodide staining.

RESULTS

Meta-analysis of rs34330 association with SLE. We used the rs34330 association results directly from the first report (3) (5,365 cases and 10,024 controls in the discovery set, with a P value for association with SLE of 5.00×10^{-13}). To replicate the genetic association of rs34330, data from 5 cohorts (4,858 cases and 8,625 controls in the replication set) were used (Supplementary Table 1, http://onlinelibrary.wiley.com/doi/10.1002/art.41799/abstract). We used direct genotyping data on rs34330 from 4 cohorts (BHC, Korean, Malayan Chinese, and European American ancestries) and augmented with summary data from a recently published report from our Japanese collaborators (13). Our results confirmed the association of rs34330 with SLE ($P = 1.71 \times 10^{-10}$) (Supplementary Table 2, http://onlinelibrary.wiley.com/doi/10.1002/art.41799/abstract).

Next, we performed a meta-analysis of the combined effect of the association of rs34330 and SLE across 11 cohorts of Asian and European ancestries (total 28,872 [10,223 cases and 18,649 controls]) (Supplementary Table 2). The results showed a strong and consistent association between rs34330 and SLE (meta-analysis $P = 5.29 \times 10^{-22}$, odds ratio 0.84 [95% confidence interval 0.81–0.87]) (Figure 2B). The odds ratios were consistent across populations with no significant heterogeneity ($I^2 = 0$, P for heterogeneity = 0.48), and the findings were confirmed to be robust when tested for publication bias, as supported by a symmetric funnel plot (Supplementary Figure 1, http://onlinelibrary.wiley.com/doi/10.1002/art.41799/abstract).

Bioinformatics prediction of rs34330 as a potential regulatory variant. Our findings of the presence of various histone marks, chromatin accessibility, and RNA Pol II occupancy all indicated that rs34330 is located within an active regulatory region (Figure 2A). Using multiple bioinformatics packages, rs34330 was scored as highly probable to be functional, based on a 3DSNP score of 163.7 (predicted as a promoter in 109 cells/tissues, 51 predicted transcription factor binding sites), a RegulomeDB score of 4 (predicted as having regulatory potential), and the presence of a ChromHMM active transcription start site (TSS).

Next, we predicted differential transcription factor binding between the risk (C) and non-risk (T) alleles of rs34330 using multiple databases, discovering several with predicted differential binding. Among these, IRFs exhibited 3–5-fold greater binding to the risk allele (Supplementary Table 3, http://onlinelibrary.wiley.com/doi/10.1002/art.41799/abstract). The transcriptional repressor CTCF bound preferentially (4–16-fold) to the non-risk allele, suggesting greater transcriptional activation at the risk allele.

Expression QTL and allele-specific expression analyses. Using several databases, we identified rs34330 as a significant eQTL, especially in immune cells (P values between 2.3×10^{-2} and $P > 1.8 \times 10^{-17}$ for several immune cell types), affecting nearby genes *APOLD1*, *DDX47*, and *GPR19* (Supplementary Table 4, http://onlinelibrary.wiley.com/doi/10.1002/art.41799/abstract). All eQTL target genes were also identified among the eQTLs assessed in Asian cohorts (21). This SNP is also an eQTL for a long noncoding RNA *RP11-59H1.4* ($P = 1.89 \times 10^{-6}$) in the whole blood of patients of Korean descent with Crohn's disease (22).

To detect allelic imbalance, we used the allele-specific expression database AlleleDB, which contains LCLs derived from individuals from the 1000 Genomes Project (28). We identified 2 heterozygous (C/T) individuals with strong allele-specific expression at rs34330. The risk allele (C)–containing *CDKN1B* transcripts were significantly greater than the non-risk allele (T)–containing transcripts in both individuals ($P = 2.15 \times 10^{-12}$ and $P = 1.22 \times 10^{-7}$, respectively).

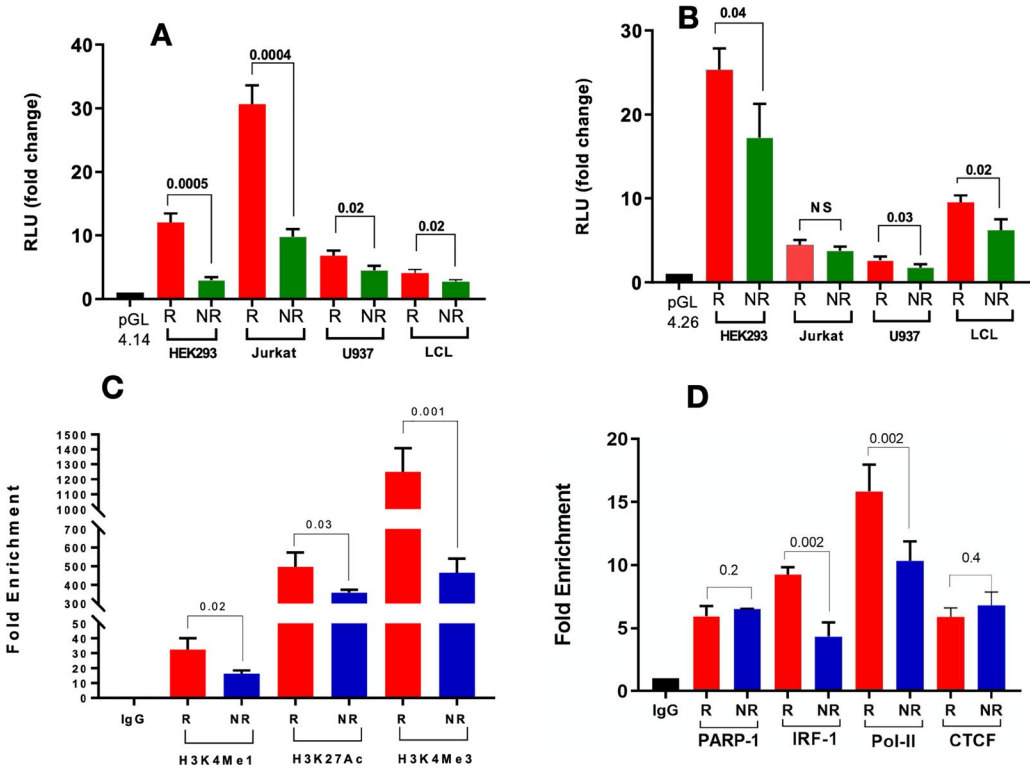

Figure 3. Results of luciferase reporter assay and chromatin immunoprecipitation (ChIP)–quantitative polymerase chain reaction (qPCR) assay for rs34330 functionality. **A**, Allele-specific promoter assays across 4 cell lines (HEK 293, Jurkat, U937, and lymphoblastoid cell lines [LCL]). **B**, Allele-specific enhancer assays across 4 cell lines (HEK 293, Jurkat, U937, and LCL). Empty vectors pGL4.14 and pGL4.26 were used as reference. **C**, ChIP-qPCR assays for determining allele-specific DNA–protein interactions with H3K4me1, H3K27ac, and H3H4me3. **D**, ChIP-qPCR assays for determining allele-specific DNA–protein interactions with poly(ADP-ribose) polymerase 1 (PARP-1), interferon regulatory factor 1 (IRF-1), RNA polymerase II (Pol II), and CCCTC-binding factor (CTCF). All analyses were conducted according to CC risk (R) and TT non-risk (NR) genotype. For each assay, the binding affinity was measured against IgG control. Bars show the mean ± SD (n = 3). Numbers above the bars are the P values, determined by Student's t-test. Primers and their sequences used for these experiments are listed in Supplementary Table 5, http://onlinelibrary.wiley.com/doi/10.1002/art.41799/abstract. RLU = relative luminescence units; NS = not significant.

Validating allele-specific regulatory effects of rs34330. To experimentally assess the allele-specific regulatory potential (promoter and enhancer) of 575-bp sequences surrounding rs34330, we used luciferase reporter assays in 4 different cell lines (HEK 293, Jurkat T lymphocytes, U937 monocytes, and LCLs [B lymphocytes]). We found marked promoter activity (up to 30-fold over empty vector) in all 4 cell lines, with the C risk allele showing significantly more activity than the T non-risk allele (~5-fold [$P = 5.0 \times 10^{-4}$] for HEK 293, ~3-fold [$P = 4.0 \times 10^{-4}$] for Jurkat, ~50% more [$P = 2.3 \times 10^{-2}$] for U937, and ~2-fold [$P = 2.0 \times 10^{-2}$] for LCLs) (Figure 3A). This is consistent with previous reports that rs34330-C exerts higher promoter activity than rs34330-T (29). Substantial enhancer activity (up to 26-fold over empty vector) was observed, using a minimal promoter plasmid (pGL4.26) with both risk-allele and non-risk allele sequence, in 3 of the 4 cell types. Sequences containing the risk allele produced significantly more reporter gene activity in HEK 293 cells (~50% more [$P = 4.15 \times 10^{-2}$]), U937 cells (~30% more [$P = 3.38 \times 10^{-2}$]), and LCLs (40% more [$P = 2.0 \times 10^{-2}$]), but not Jurkat cells ($P = 0.188$), indicating that the rs34330-C base is critical for enhancer activity in a cell type–dependent manner (Figure 3B).

Allele-specific binding of rs34330 to regulatory proteins. Since the region containing rs34330 colocalizes with strong promoter and enhancer activity, we sought to identify interacting proteins. Two Coriell cell lines with risk and non-risk genotypes were used for these experiments. First, using ChIP-grade antibodies (Abcam), we checked histone marks H3K27ac and H3K4me3, which are usually associated with active transcription near the promoter/transcription start site, and H3K4me1, which is usually associated with active transcription at an enhancer. As expected, we observed significantly more active marking with the CC genotype (risk) than the TT genotype (non-risk) (~2-fold [$P = 2.2 \times 10^{-2}$] for H3K4me1, ~1.6-fold [$P = 3.92 \times 10^{-2}$] for H3K27ac, and ~3-fold [$P = 1.4 \times 10^{-3}$] for H3K4me3) (Figure 3C), with the 2 most

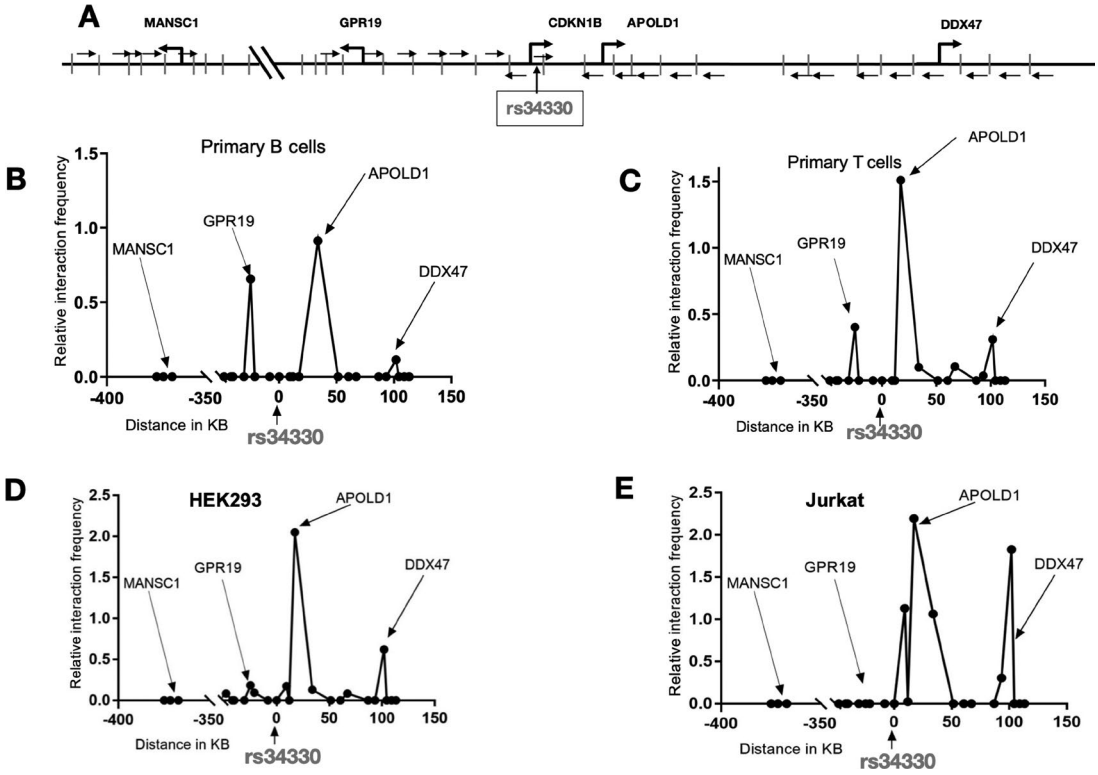

Figure 4. Long-range chromosomal interaction analysis of the rs34330 region using chromosome conformation capture. **A**, Schematic representation of the rs34330 region with primer locations for chromosome conformation capture experiments and neighboring gene regions. Vertical lines indicate the position of *Sac* I restriction enzyme sites. **Small arrows** represent the primer location with orientation. The forward primer at the rs34330 region is the common primer for all other reverse primers within the *APOLD1* and *DDX47* gene regions. Similarly, the reverse primer at the rs34330 region is the common primer for all other forward primers within the *GPR19* and *MANSC1* gene regions. **Large arrows** represent the transcriptional start site of the respective genes. **B–E**, Relative interaction of rs34330 regions with different genomic regions in primary B cell lines (**B**), primary T cell lines (**C**), HEK 293 cell lines (**D**), and Jurkat cell lines (**E**). The relative interaction frequency for each primer set represents the intensity of the polymerase chain reaction band from experimental DNA normalized to the polymerase chain reaction band intensity from bacterial artificial chromosome DNA. The x-axis shows the genomic distance of the interacting region in the forward and reverse directions from single-nucleotide polymorphism rs34330 (0 kb). Circles represent the relative interaction frequencies at the corresponding restriction sites. Primers and their sequences used for these experiments are listed in Supplementary Table 5, http://onlinelibrary.wiley.com/doi/10.1002/art.41799/abstract.

significant marks being the promoter/TSS-associated modifications (H3K4me1 and H3K4me3), consistent with the location of rs34330.

Next, we tested the differential binding of the transcription factors predicted through bioinformatics. Antibodies against Pol II bound significantly more with the risk genotype (~50% more; $P = 2.11 \times 10^{-3}$) than the non-risk genotype, consistent with greater transcriptional activity of the risk allele. As it was predicted by bioinformatics analysis that several IRF transcription factors could differentially bind to the SNP region (Supplementary Table 3, http://onlinelibrary.wiley.com/doi/10.1002/art.41799/abstract), we tested IRFs 2, 4, 5, and 8, but did not detect any binding at this region (data not shown). However, IRF-1 showed strong binding, with ~2-fold as much at the risk locus ($P = 2.5 \times 10^{-3}$). With post hoc annotation of the SNP region using ConSite (30), we identified a plausible IRF-1 site 27 bp away from the SNP (Supplementary Figure 2, http://onlinelibrary.wiley.com/doi/10.1002/art.41799/abstract). SNP effects on transcription factor binding sites that are within close proximity are routinely observed (31), manifested through mechanisms such as protein–protein interactions with the transcription factor, alteration of histone occupancy, or mediators of chromatin looping. To assess differential binding with CTCF, we tested for binding that was significantly enriched around the rs34330 region compared to IgG. Relatively greater binding was found with the non-risk allele compared to the risk allele (as suggested in the bioinformatics analysis), but the difference was not significant ($P = 0.4$) (Figure 3D).

In addition to testing the predicted transcription factors, we pursued an unbiased approach to discovering binding proteins, using a DNA pull-down assay followed by an EMSA. This revealed an ~100-kd band preferentially binding to the risk allele; mass spectrometry of this band identified PARP-1 as the binding protein (Supplementary Figure 3, http://onlinelibrary.wiley.com/doi/10.1002/art.41799/abstract). Follow-up experiments with ChIP-qPCR showed substantial binding to both the risk and non-risk alleles, with no allelic differences (Figure 3D). The source of the apparent discrepancy in findings between the 2 techniques is not known and may involve cell type–specific effects (Jurkat cells for EMSA and Coriell LCLs for ChIP-qPCR).

Long-range chromatin interactions between rs34330 and target genes. To examine interactions between the rs34330 region and neighboring promoters, we performed chromosome conformation capture experiments in primary T cells, B cells, HEK 293 cells, and Jurkat cells, using semiquantitative PCR (Figure 4A). We detected interaction between rs34330 and the *APOLD1* and *DDX47* promoters in all 4 cell lines tested

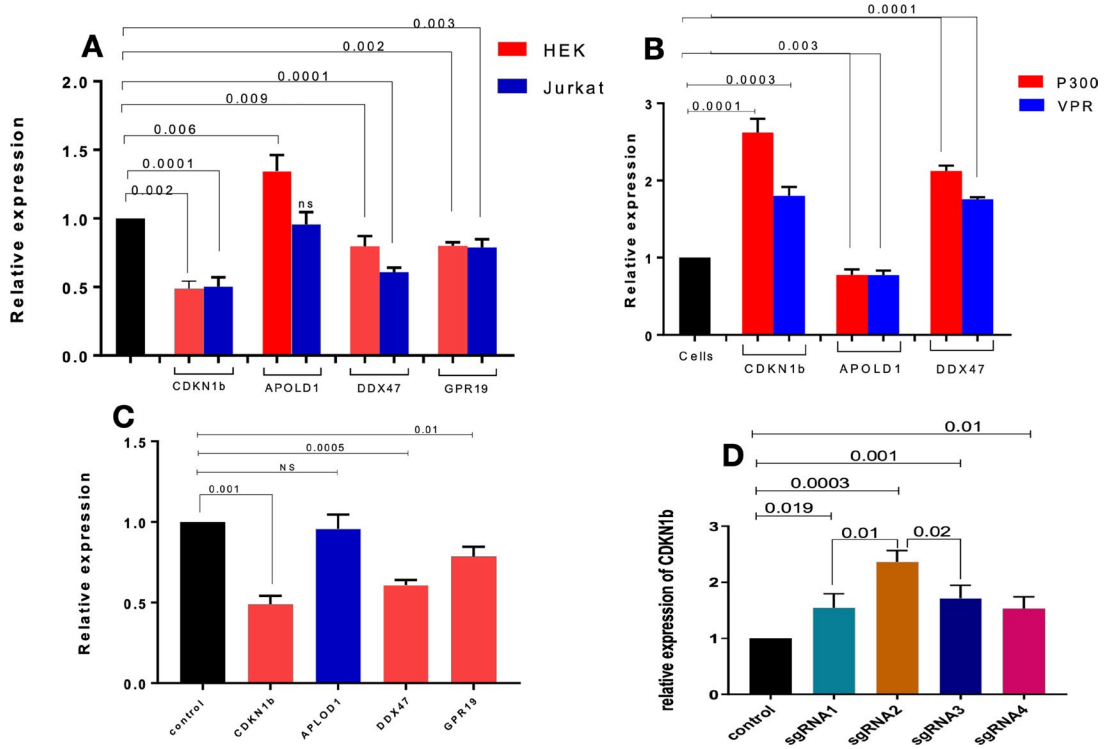

Figure 5. Effects of clustered regularly interspaced short palindromic repeat (CRISPR)–based genetic and epigenetic editing in different study models. **A**, Levels of mRNA for *CDKN1B*, *APOLD1*, and *DDX47* in pooled edited cells. **B**, Epigenetic effects of CRISPR-based activation on *CDKN1B*, *APOLD1*, and *DDX47* using dCas9-p300 and dCas9-VPR in HEK 293 cells. **C**, Epigenetic effects of CRISPR inhibition using dCas9-KRAB-MeCP2 in HEK 293 cells. **D**, Epigenetic fine-mapping of rs34330 relative to the transcriptional functional unit for *CDKN1B* expression using dCas9-p300. Numbers above the bars are the *P* values, determined by Student's *t*-test. Bars show the mean ± SD (n = 3). NS = not significant; sgRNA = single-guide RNA. Primers and their sequences used for these experiments are listed in Supplementary Table 5, http://onlinelibrary.wiley.com/doi/10.1002/art.41799/abstract.

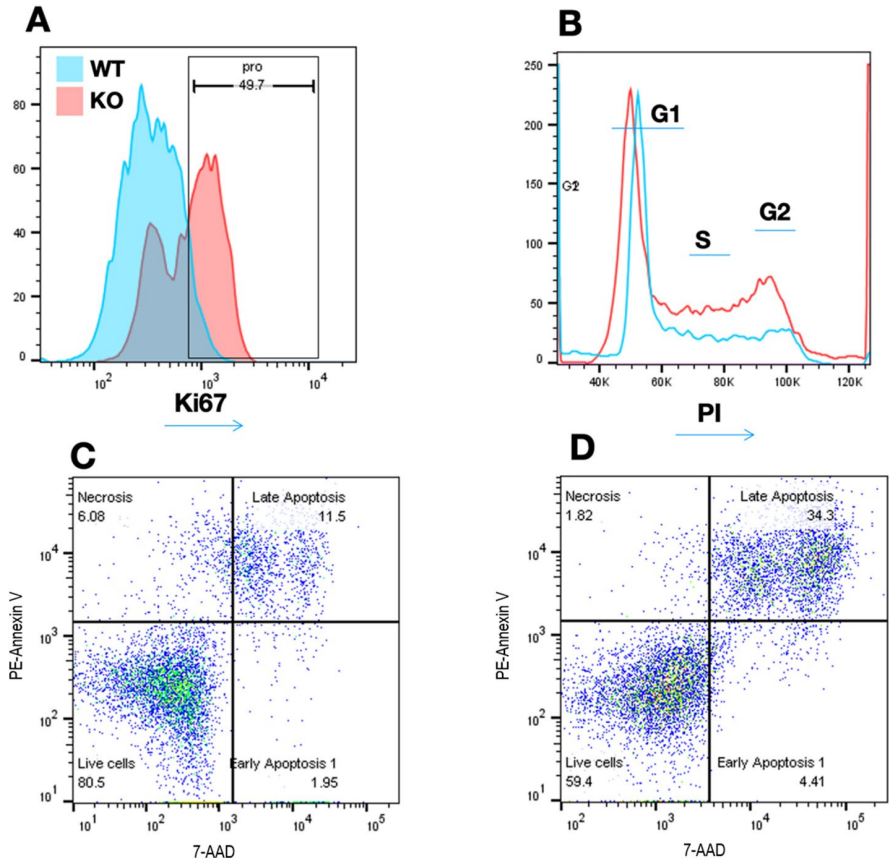

Figure 6. Flow cytometry analysis for assessing proliferation and apoptosis of clustered regularly interspaced short palindromic repeat (CRISPR)–edited Jurkat cell lines. **A**, Ki-67 staining in wild-type (WT) Jurkat cells versus CRISPR-edited knockout (KO) Jurkat cells, showing high proliferation (pro) in KO cells (red) compared to WT cells (blue). **B**, Cell cycle analysis performed with propidium iodide (PI) staining of KO cells (red) versus WT cells (blue), showing highly increased levels of S phase and G_2 phase. **C** and **D**, Flow cytometry charts showing apoptosis measured by staining with phycoerythrin (PE)–conjugated annexin V/7-aminoactinomycin D (7-AAD). The percentage of apoptotic cells was determined in WT cells (**C**) and KO cells (**D**).

(Figures 4B–E). Chromosome conformation capture cannot discriminate *CDKN1B* promoter binding, as it is only 79 bp away. Interactions with the *DDX47* promoter were higher in Jurkat cells than HEK 293 cells, indicating cell type–specific interactions or chromatin states of this region. Thus, the rs34330 region predominantly interacts with the *DDX47* and *APOLD1* promoters, consistent with the eQTL results in which these 2 genes were the most significantly modulated. While no significant interaction with the *MANSC1* promoter regions was detected in any cells, interaction with *GPR19* was detected in both primary B cells and T cells.

Validating transcriptional impacts of rs34330 on target genes using CRISPR-based genome editing. To validate the observed transcriptional effects of the rs34330 region, we deleted ~35 bases in HEK 293 and Jurkat cells with CRISPR/Cas9 (32), using a pool of 3 sgRNAs. We confirmed ~35 bp deletion by Sanger sequencing. The editing efficiency was very high: 98% for HEK 293 cells and 87% for Jurkat cells (Supplementary Figure 4, http://onlinelibrary.wiley.com/doi/10.1002/art.41799/abstract). Next, we performed qRT-PCR on WT and CRISPR/Cas9-edited (KO) HEK 293 and Jurkat cells. Levels of *CDKN1B*, *DDX47*, and *GPR19* were significantly reduced in KO cells (~50% [$P = 2.0 \times 10^{-3}$], ~25% [$P = 9.0 \times 10^{-3}$], and ~25% [$P = 2.0 \times 10^{-3}$], respectively, in HEK 293 cells and ~50% [$P = 1.0 \times 10^{-4}$], ~40% [$P = 1.0 \times 10^{-4}$], and ~25% [$P = 3.0 \times 10^{-3}$], respectively, in Jurkat cells) (Figure 5A). Interestingly, *APOLD1* was up-regulated in KO HEK 293 cells (~35% [$P = 6.0 \times 10^{-3}$]), but not in Jurkat cells ($P = 4.5 \times 10^{-1}$). These observations confirm that rs34330 has cell type–specific repressive and enhancing effects on *CDKN1B* and nearby genes.

Epigenetic modification of the rs34330 region. CRISPR/Cas9 can be converted into a targetable transcriptional activator or repressor, permitting mechanistic epigenetic studies of gene loci (25). We performed CRISPR/dCas9-based activation using 2 transcriptional modulator domains, one performing histone acetylation with a histone acetyltransferase (dCas9-p300)

and another recruiting transcription complexes to the promoter with the HIV-derived VPR activator (dCas9-VPR) (25). We also used CRISPR/dCas9-based inhibition with the hybrid repressor protein Kruppel-associated box (KRAB)–methyl-CpG binding protein 2 (MeCP-2). Epigenetic activation with P300 and VPR increased expression of *CDKN1B* ~2–3-fold, along with *DDX47* (~2-fold), in HEK 293 cells, whereas *APOLD1* expression was significantly reduced (~20%) (Figure 5B). The KRAB-MeCP-2 repressor significantly decreased *CDKN1B* expression in HEK 293 cells by ~2-fold, *DDX47* by ~40%, and *GPR19* by ~30%; *APOLD1* was unaffected (Figure 5C).

Next, to determine the importance of sgRNA position with respect to rs34330, we measured *CDKN1B* expression using sgRNA-based activation with dCas9-p300. We found that all 4 sgRNAs significantly increased *CDKN1B* expression. The greatest expression increase was from sgRNA2 (12 bases from rs34330), increasing expression ~40% more than was observed with the other sgRNAs (Figure 5D).

Impact of the rs34330 region on apoptosis and proliferation. Cyclins, CDKs, and CDK inhibitors, including CDKN1B/p27^{Kip1}, play crucial roles in the cell cycle and cellular proliferation. These proteins regulate transitions between the G_1, S, G_2, and M cell cycle phases, especially the G_1 to S phase (33). Cell cycle progression is usually inhibited by p27^{Kip1} (7), primarily by blocking CDK-2/cyclin E complex activation. We sought to determine the effect of the rs34330 region on apoptosis and proliferation, using the WT and KO cells described above. Cell cycle progression was monitored with propidium iodide staining of DNA, proliferation was assessed by immunolabeling against Ki-67, and apoptosis was investigated by staining of DNA with 7-aminoactinomycin D (7-AAD) and anti–annexin V antibodies. A substantial increase in Ki-67 staining (50%) was seen in KO Jurkat cells compared to WT Jurkat cells (Figure 6A). The number of cells at the G_1 to G_2 division dramatically increased in KO cells (Figure 6B). Upon serum starvation, KO cells showed much greater annexin V/7-AAD staining than WT cells (35% versus 11%) (Figures 6C and D). Thus, KO cells showed much higher levels of proliferation, cell cycle progression, and apoptosis than WT cells, suggesting that the rs34330 region played a prominent role in suppressing these 3 phenomena, likely through regulation of p27^{Kip1} levels.

DISCUSSION

Converting GWAS data on complex traits into mechanistic understanding of the underlying pathologic processes presents a formidable challenge (34). *CDKN1B* (i.e., p27^{Kip1} and Kip1) has been proposed as an SLE susceptibility locus in Asian populations (3). However, this association result has not yet been thoroughly studied, nor have underlying mechanisms been defined or any target gene(s) of this genetic association been proposed. In this study, we replicated a genetic association between SLE and rs34330 and established several aspects of the mechanism of its contribution to disease.

SLE is accompanied by dysregulated activation and proliferation of immune cells, primarily T cells and B cells. An intricate balance of cyclins, CDKs, and CDK inhibitors (e.g., p27^{Kip1}) regulates cell cycle progression, activation, proliferation, autophagy, and apoptosis in these cells, and genetic lesions can disrupt these pathways. Increasing evidence has shown that immune cell abnormalities, dysregulated apoptosis, and poor clearance of apoptotic and autophagic materials can contribute to SLE development and progression.

CDKN1B encodes p27^{Kip1}, an inhibitor of cyclin/CDK complexes, which are crucial for cell cycle progression and development (4,5). Dysregulated expression of p27^{Kip1} is a frequent event in several human cancers (7). *CDKN1B* has 2 paralogs in the genome, *CDKN1A* (encoding p21^{Waf1}) and *CDKN1C* (encoding p57^{Kip2}), with related functions in cell cycle regulation, proliferation, and apoptosis (35). Reduced expression of *CDKN1A* is associated with SLE susceptibility, and the 5′-UTR SNP rs762624 is linked to risk of both SLE and lupus nephritis (36). Moreover, interferon-1–mediated induction of p21^{Waf1} contributes to induction of apoptosis (37). Apoptosis is inhibited by binding of p57^{Kip2} to the stress-related kinase MAPK8. We have previously shown that rs1990760, the SLE risk allele of *IFIH1*, drove inflammatory signaling in part, leading to increased transcription of *MAPK8* (38). Autoantibodies against p57^{Kip2} are frequently observed in neonatal lupus, particularly in conjunction with anti-Ro antibodies (39). Thus, all 3 members of the *CDKN1* (also known as Cip/Kip) family have demonstrated SLE involvement.

In this study, we replicated the association of rs34330 in 4 additional Asian cohorts and in a European cohort. We also subsequently proposed and experimentally validated a potential mechanism underlying SLE pathogenicity. The rs34330 variant is located in a region of active chromatin upstream (–79 bp) of the *CDKN1B* translation start site, with potential for both promoter and enhancer activity. Our analysis supports the notion that rs34330 is an eQTL for multiple neighboring genes, *APOLD1* in particular. Luciferase reporter assays using a 575-bp sequence surrounding rs34330 confirmed allele-specific promoter (HEK 293, Jurkat, and U937) and enhancer (HEK and U937) activities, with the risk allele (C) having significantly higher promoter and enhancer activity than the non-risk allele (T). ChIP-qPCR showed allele-specific binding to IRF-1 and Pol II, as well as several active histone marks (H3K4me1, H3K27ac, and H3K4me3). IRF-1 is a critical immune transcription factor, with implications in numerous autoimmune diseases. It drives inflammasome hyperactivity in SLE, is a dendritic cell marker for SLE progression (40), and is a potent transcriptional activator of major histocompatibility complex class I genes (41), among many other targets.

We applied several approaches to identify target genes and mechanisms underlying the rs34330 association. First, we used chromosome conformation capture experiments to detect

regions of chromatin looping, bringing together promoters and enhancers. Our chromosome conformation capture experiments showed a significant interaction between the rs34330 region and *APOLD1*, *GPR19*, and *DDX47*. Second, to functionally detect target genes, we used CRISPR/Cas9 to delete ~35 bases surrounding rs34330. KO cells showed *APOLD1* up-regulation and *CDKN1B*, *GPR19*, and *DDX47* down-regulation. Third, we used CRISPR-based activation and CRISPR inhibition–based epigenetic activation and silencing. The up-regulation of *APOLD1* and down-regulation of *CDKN1B*, *DDX47*, and *GPR19* were reproduced with the two approaches. *GPR19* is similarly involved in both cell cycle progression (particularly G_2/M) (42) and apoptosis (43), and rs34330 may regulate these processes by changing levels of both $p27^{Kip1}$ and *GPR19*. *DDX47* is a DEAD box RNA helicase, many of which are involved in innate immunity, with some being known SLE risk genes, including *IFIH1/MDA5*, *RIG1/DDX58*, and *LGP2/DHX58*, as well as their adaptor mitochondrial antiviral signaling protein (44). Further studies are required to more finely dissect the effects of rs34330 on *CDKN1B*, *APOLD1*, *DDX47*, and *GPR19* contributing to SLE susceptibility.

We cannot rule out the involvement of other biochemical pathways not explored in our study. Notably, $p27^{Kip1}$ plays other roles in immune function, for instance in regulating T cell anergy (inadequate T cell costimulation despite antigen recognition) (41). Systemic autoimmunity was also inhibited by $p27^{Kip1}$ through control of Treg cell activity and differentiation (45). Deficiency of $p27^{Kip1}$ in aged C57BL/6 mice reduced the number and activity of Treg cells and induced the development of mild lupus-like abnormalities, indicating that the SLE association of *CDKN1B* may be due, at least in part, to immune phenotypes not directly queried in this study (45). However, no studies in humans have been reported.

Despite the strong genetic association of rs34330, and our experiments directly evaluating the effect of this single-basepair change on enhancer and promoter activity, gene expression, and binding of active histone marks and transcriptional activators (as well as a direct validation of the effects of the ~35-bp rs34330 region on apoptosis, proliferation, and cell cycle progression), we cannot rule out the possibility that there may be other functional SNPs in this locus. Interestingly, no SNPs with a linkage disequilibrium (LD) threshold of $r^2 = 0.6$ were found in our study populations of Asian ancestry (Supplementary Table 6, available on the *Arthritis & Rheumatology* website at http://onlinelibrary.wiley.com/doi/10.1002/art.41799/abstract). At a relaxed LD threshold, we found several SNPs around rs34330. However, the closest top and bottom SNPs were far away ($r^2 = 0.55$ [distance 759 bases] for rs36228499 and $r^2 = 0.42$ [distance 2,958 bases] for rs34324). As rs34330-deleted KO cells had many relevant phenotypes, we can at least accept the rs34330 region as a functional regulatory unit.

Taken together, our findings show that the risk rs34330 C allele exhibits increased binding with the IRF-1 transcriptional activator, and Pol II is associated with significant increases in 3 active chromatin marks, has potent promoter activity (~3–5 times more than the non-risk allele) and enhancer activity (~40% more than the non-risk allele), is physically associated with the *APOLD1* and *DDX47* promoters (in addition to being located in the *CDKN1B* promoter), and drives increased expression of *CDKN1B*, *DDX47*, and *GPR19* and decreased expression of *APOLD1*. Increased occupancy of CTCF around rs34330 supports its role, but it is unclear whether CTCF affects allele-specific gene expression through its looping. The region surrounding the SNP was also shown to negatively regulate proliferation, cell cycle progression, and apoptosis, as evidenced from studies on KO cells. This study demonstrates the effectiveness of hypothesis-driven follow-up experiments to conclusively localize GWAS association with specific SNPs and their associated mechanisms.

ACKNOWLEDGMENTS

We thank all patients with SLE and healthy controls who participated in this study. We also thank the research assistants, coordinators, and physicians who helped in the recruitment of subjects for this project.

AUTHOR CONTRIBUTIONS

All authors were involved in drafting the article or revising it critically for important intellectual content, and all authors approved the final version to be published. Dr. Singh had full access to all of the data in the study and takes responsibility for the integrity of the data and the accuracy of the data analysis.

Study conception and design. Singh, Maiti, Nath.

Acquisition of data. Singh, Maiti, Zhou, Bae, Terao, Okada, Chua, Kochi, Zhang, Nath.

Analysis and interpretation of data. Singh, Maiti, Fazel-Najafabadi, Sun, Guthridge, Weirauch, James, Harley, Varshney, Looger, Nath.

REFERENCES

1. Alarcón-Riquelme ME, Ziegler JT, Molineros J, Howard TD, Moreno-Estrada A, Sánchez-Rodríguez E, et al. Genome-wide association study in an Amerindian ancestry population reveals novel systemic lupus erythematosus risk loci and the role of European admixture. Arthritis Rheumatol 2016;68:932–43.
2. Oparina N, Martinez-Bueno M, Alarcon-Riquelme ME. An update on the genetics of systemic lupus erythematosus [review]. Curr Opin Rheumatol 2019;31:659–68.
3. Yang W, Tang H, Zhang Y, Tang X, Zhang J, Sun L, et al. Meta-analysis followed by replication identifies loci in or near CDKN1B, TET3, CD80, DRAM1, and ARID5B as associated with systemic lupus erythematosus in Asians. Am J Hum Genet 2013;92:41–51.
4. Bencivenga D, Caldarelli I, Stampone E, Mancini FP, Balestrieri ML, Della Ragione F, et al. $p27^{Kip1}$ and human cancers: a reappraisal of a still enigmatic protein [review]. Cancer Lett 2017;403:354–65.
5. Sherr CJ, Roberts JM. CDK inhibitors: positive and negative regulators of G_1-phase progression [review]. Genes Dev 1999;13:1501–12.
6. Larrea MD, Hong F, Wander SA, da Silva TG, Helfman D, Lannigan D, et al. RSK1 drives $p27^{Kip1}$ phosphorylation at T198 to promote RhoA inhibition and increase cell motility. Proc Natl Acad Sci U S A 2009;106:9268–73.
7. Yang Q, Al-Hendy A. The emerging role of p27 in development of diseases. Cancer Stud Mol Med 2018;4:e1–3.
8. Jia W, He MX, McLeod IX, Guo J, Ji D, He YW. Autophagy regulates T lymphocyte proliferation through selective degradation of the cell-cycle inhibitor CDKN1B/p27Kip1. Autophagy 2015;11:2335–45.

9. Cheng XK, Wang XJ, Li XD, Ren XQ. Genetic association between the cyclin-dependent kinase inhibitor gene p27/Kip1 polymorphism (rs34330) and cancer susceptibility: a meta-analysis. Sci Rep 2017;7:44871.
10. Tan W, Gu Z, Shen B, Jiang J, Meng Y, Da Z, et al. PTEN/Akt-p27^{kip1} signaling promote the BM-MSCs senescence and apoptosis in SLE patients. J Cell Biochem 2015;116:1583–94.
11. Willer CJ, Li Y, Abecasis GR. METAL: fast and efficient meta-analysis of genomewide association scans. Bioinformatics 2010;26:2190–1.
12. Sun C, Molineros JE, Looger LL, Zhou XJ, Kim K, Okada Y, et al. High-density genotyping of immune-related loci identifies new SLE risk variants in individuals with Asian ancestry. Nat Genet 2016;48:323–30.
13. Akizuki S, Ishigaki K, Kochi Y, Law SM, Matsuo K, Ohmura K, et al. PLD4 is a genetic determinant to systemic lupus erythematosus and involved in murine autoimmune phenotypes. Ann Rheum Dis 2019;78:509–18.
14. Purcell S, Neale B, Todd-Brown K, Thomas L, Ferreira MA, Bender D, et al. PLINK: a tool set for whole-genome association and population-based linkage analyses. Am J Hum Genet 2007;81:559–75.
15. Ward LD, Kellis M. HaploReg: a resource for exploring chromatin states, conservation, and regulatory motif alterations within sets of genetically linked variants. Nucleic Acids Res 2012;40:D930–4.
16. Lu Y, Quan C, Chen H, Bo X, Zhang C. 3DSNP: a database for linking human noncoding SNPs to their three-dimensional interacting genes. Nucleic Acids Res 2017;45:D643–9.
17. Boyle AP, Hong EL, Hariharan M, Cheng Y, Schaub MA, Kasowski M, et al. Annotation of functional variation in personal genomes using RegulomeDB. Genome Res 2012;22:1790–7.
18. Grundberg E, Small KS, Hedman AK, Nica AC, Buil A, Keildson S, et al. Mapping cis- and trans-regulatory effects across multiple tissues in twins. Nat Genet 2012;44:1084–9.
19. Carithers LJ, Moore HM. The Genotype-Tissue Expression (GTEx) project [editorial]. Biopreserv Biobank 2015;13:307–8.
20. Westra HJ, Peters MJ, Esko T, Yaghootkar H, Schurmann C, Kettunen J, et al. Systematic identification of trans eQTLs as putative drivers of known disease associations. Nat Genet 2013;45:1238–43.
21. Narahara M, Higasa K, Nakamura S, Tabara Y, Kawaguchi T, Ishii M, et al. Large-scale East-Asian eQTL mapping reveals novel candidate genes for LD mapping and the genomic landscape of transcriptional effects of sequence variants. PLoS One 2014;9:e100924.
22. Jung S, Liu W, Baek J, Moon JW, Ye BD, Lee HS, et al. Expression quantitative trait loci (eQTL), apping in Korean patients with Crohn's disease and identification of potential causal genes through integration with disease associations. Front Genet 2020;11:486.
23. Jansen R, Hottenga JJ, Nivard MG, Abdellaoui A, Laport B, de Geus EJ, et al. Conditional eQTL analysis reveals allelic heterogeneity of gene expression. Hum Mol Genet 2017;26:1444–51.
24. Molineros JE, Singh B, Terao C, Okada Y, Kaplan J, McDaniel B, et al. Mechanistic characterization of RASGRP1 variants identifies an hnRNP-K-regulated transcriptional enhancer contributing to SLE susceptibility. Front Immunol 2019;10:1066.
25. Chavez A, Scheiman J, Vora S, Pruitt BW, Tuttle M, Iyer EP, et al. Highly efficient Cas9-mediated transcriptional programming. Nat Methods 2015;12:326–8.
26. Hilton IB, D'Ippolito AM, Vockley CM, Thakore PI, Crawford GE, Reddy TE, et al. Epigenome editing by a CRISPR-Cas9-based acetyltransferase activates genes from promoters and enhancers. Nat Biotechnol 2015;33:510–7.
27. Yeo NC, Chavez A, Lance-Byrne A, Chan Y, Menn D, Milanova D, et al. An enhanced CRISPR repressor for targeted mammalian gene regulation. Nat Methods 2018;15:611–6.
28. Chen J, Rozowsky J, Galeev TR, Harmanci A, Kitchen R, Bedford J, et al. A uniform survey of allele-specific binding and expression over 1000-Genomes-Project individuals. Nature Commun 2016;7:11101.
29. Capasso M, McDaniel LD, Cimmino F, Cirino A, Formicola D, Russell MR, et al. The functional variant rs34330 of CDKN1B is associated with risk of neuroblastoma. J Cell Mol Med 2017;21:3224–30.
30. Sandelin A, Wasserman WW, Lenhard B. ConSite: web-based prediction of regulatory elements using cross-species comparison. Nucleic Acids Res 2004;32:W249–52.
31. MacQuarrie KL, Fong AP, Morse RH, Tapscott SJ. Genome-wide transcription factor binding: beyond direct target regulation [review]. Trends Genet 2011;27:141–8.
32. Mali P, Yang L, Esvelt KM, Aach J, Guell M, DiCarlo JE, et al. RNA-guided human genome engineering via Cas9. Science 2013;339:823–6.
33. Kawamata N, Morosetti R, Miller CW, Park D, Spirin KS, Nakamaki T, et al. Molecular analysis of the cyclin-dependent kinase inhibitor gene p27/Kip1 in human malignancies. Cancer Res 1995;55:2266–9.
34. Claussnitzer M, Cho JH, Collins R, Cox NJ, Dermitzakis ET, Hurles ME, et al. A brief history of human disease genetics. Nature 2020;577:179–89.
35. Wan Q, Chen H, Li X, Yan L, Sun Y, Wang J. Artesunate inhibits fibroblasts proliferation and reduces surgery-induced epidural fibrosis via the autophagy-mediated p53/p21(waf1/cip1) pathway. Eur J Pharmacol 2019;842:197–207.
36. Kim K, Sung YK, Kang CP, Choi CB, Kang C, Bae SC. A regulatory SNP at position -899 in CDKN1A is associated with systemic lupus erythematosus and lupus nephritis. Genes Immun 2009;10:482–6.
37. Papageorgiou A, Dinney CP, McConkey DJ. Interferon-α induces TRAIL expression and cell death via an IRF-1-dependent mechanism in human bladder cancer cells. Cancer Biol Ther 2007;6:872–9.
38. Molineros JE, Maiti AK, Sun C, Looger LL, Han S, Kim-Howard X, et al. Admixture mapping in lupus identifies multiple functional variants within IFIH1 associated with apoptosis, inflammation, and autoantibody production. PLoS Genet 2013;9:e1003222.
39. Niewold TB, Rivera TL, Buyon JP, Crow MK. Serum type I interferon activity is dependent on maternal diagnosis in anti-SSA/Ro–positive mothers of children with neonatal lupus. Arthritis Rheum 2008;58:541–6.
40. Wardowska A, Komorniczak M, Bułło-Piontecka B, Dębska-Ślizień MA, Pikuła M. Transcriptomic and epigenetic alterations in dendritic cells correspond with chronic kidney disease in lupus nephritis. Front Immunol 2019;10:2026.
41. Chang CH, Hammer J, Loh JE, Fodor WL, Flavell RA. The activation of major histocompatibility complex class I genes by interferon regulatory factor-1 (IRF-1). Immunogenetics 1992;35:378–84.
42. Kastner S, Voss T, Keuerleber S, Glockel C, Freissmuth M, Sommergruber W. Expression of G protein-coupled receptor 19 in human lung cancer cells is triggered by entry into S-phase and supports G(2)-M cell-cycle progression. Mol Cancer Res 2012;10:1343–58.
43. Huang L, Guo B, Liu S, Miao C, Li Y. Inhibition of the LncRNA Gpr19 attenuates ischemia-reperfusion injury after acute myocardial infarction by inhibiting apoptosis and oxidative stress via the miR-324-5p/Mtfr1 axis. IUBMB Life 2020;72:373–83.
44. Oliveira L, Sinicato NA, Postal M, Appenzeller S, Niewold TB. Dysregulation of antiviral helicase pathways in systemic lupus erythematosus [review]. Front Genet 2014;5:418.
45. Iglesias M, Postigo J, Santiuste I, González J, Buelta L, Tamayo E, et al. p27^{Kip1} inhibits systemic autoimmunity through the control of Treg cell activity and differentiation. Arthritis Rheum 2013;65:343–54.